Towards an extended algebraic variational multiscale-multigrid method for turbulent premixed combustion based on a combined G-equation/progress-variable approach

By V. Gravemeier†

1. Motivation and objectives

Turbulent premixed combustion is widely considered as being inherently more complex than turbulent non-premixed combustion because of the much stronger coupling between chemistry and turbulence; see, e.g., Bilger *et al.* (2005). Large-Eddy Simulation (LES) appears to be particularly promising for premixed combustion problems, since it explicitly resolves the large-scale unsteady motions which play a significant role when the reactants are premixed. However, LES of turbulent combustion represents a relatively new research field, which started to develop at the end of the 1990s. Review articles on LES of turbulent combustion were recently published (e.g., Janicka & Sadiki (2005); Pitsch (2006)). A particular problem related to LES of premixed combustion is the fact that the flame very often is at a computationally entirely unresolvable scale. Two popular (geometrical) modeling concepts are the following: one is based on a progress-variable equation (or c-equation) and another is based on the G-equation. Both concepts are usually considered within the laminar flamelet concept; see, e.g., Peters (2000).

According to Pitsch (2006), the G-equation concept as proposed by Williams (1985) is a numerical method to overcome the problem of flame resolution rather than a model. It is usually applied in the context of a level-set approach; see, e.g., Osher & Fedkiw (2003) for level-set methods. The progress-variable concept in the form of a flame-surface-density (FSD) approach was used for LES, for instance, in Boger *et al.* (1998); Hawkes & Cant (2000). Recently, a new procedure was proposed in Moureau *et al.* (2009), jointly using the progress-variable and G-equation concept. The motivation for developing this joint modeling procedure was the fact that, although most of the time the thickness of the flame front is much smaller than the characteristic discretization length, the flame front may be thickened by turbulence effects such that it is in the range of or even larger than the characteristic discretization length in the thin-reaction-zones regime. In such cases, the G-equation concept is rather inappropriate, whereas the progress-variable concept usually suffers from resolution deficiencies in the majority of the other cases. As a remedy, a joint modeling procedure was proposed in Moureau *et al.* (2009) and later also used in Hartmann *et al.* (2010). For this procedure to work properly, the solutions to progress-variable and G-equation must always be consistent. For this purpose, a compatibility condition was formulated in Moureau *et al.* (2009); a slightly modified condition was given in Hartmann *et al.* (2010).

† current address: Emmy Noether Research Group "Computational Multiscale Methods for Turbulent Combustion", Technische Universität München, Boltzmannstr. 15, D-85748 Garching, Germany, e-mail: vgravem@lnm.mw.tum.de

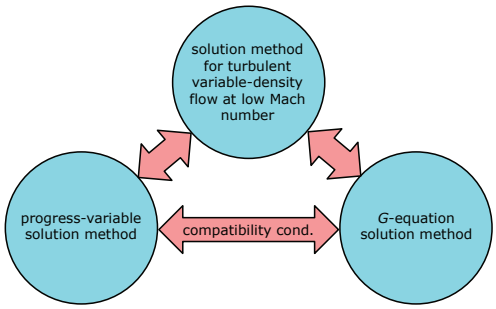

FIGURE 1. Sketch of principal arrangement of solution methods.

In preceding work, the foundation for the present work was established by developing the following computational methods:

- an algebraic variational multiscale-multigrid method (AVM^3) for large-eddy simulation of turbulent variable-density flow at low Mach number in Gravemeier & Wall (2010*a*),
- an eXtended Finite Element Method (XFEM) based on the *G*-equation concept for premixed combustion in van der Bos & Gravemeier (2009),
- an XFEM with a different type of enrichment function for two-phase flow problems in Rasthofer *et al.* (2010), and
- a further methodical development of the AVM^3, among others, towards a progress-variable approach to premixed combustion in Gravemeier & Wall (2010*b*).

The reader is referred to those articles for elaborate descriptions of the methods as well as results from various test problems achieved with the respective methods.

The goal of the present Research Brief, which reflects the main focus of the author's work during his research stay at the Center for Turbulence Research, is the theoretical development of a comprehensive framework encompassing the aforementioned methodical approaches, AVM^3 and XFEM. The method arising from this framework may accordingly be named XAVM^3. In particular, a computational method in the spirit of the combined *G*-equation/progress-variable modeling approach as originally proposed in Moureau *et al.* (2009) is intended to be made available. Of course, both individual modeling concepts will also still be available, and it may be decided on the most appropriate modeling concept for the given problem configuration within the actual computation based on characteristic values as described below. The principal arrangement of the solution methods including the compatibility condition ensuring the solution of progress-variable and *G*-equation to be "sychronous" is sketched in Fig. 1. Some of our current research activities which are concerned with further improvements of the XFEM based on the *G*-equation concept and required for the combined concept as well will be addressed in Section 3.

Similar to all of the aforementioned individual approaches, the present framework is based on finite element procedures; to the best of the author's knowledge, this as well as the preceding work are the first attempts to develop finite-element-based computational methods for the specific problem of turbulent premixed combustion. It will represent a key part of the multiscale-multiphysics software platform BACI, developed and maintained by the Institute of Computational Mechanics at the Technische Universität München, at which the author's Emmy Noether research group resides.

2. Results

2.1. *Governing equations*

Mass, momentum, G- and progress-variable equations in the problem domain Ω under the assumption of flow at low Mach number are given as follows:

$$\frac{\partial \rho}{\partial t} + \nabla \cdot (\rho \mathbf{u}) = 0, \tag{2.1}$$

$$\rho \frac{\partial \mathbf{u}}{\partial t} + \rho \mathbf{u} \cdot \nabla \mathbf{u} + \nabla p_{\mathrm{hyd}} - \nabla \cdot \left(2\mu \varepsilon' (\mathbf{u})\right) = \rho \mathbf{g}, \tag{2.2}$$

$$\rho \frac{\partial G}{\partial t} + \rho \mathbf{u} \cdot \nabla G + \rho_{\mathrm{u}} \left(s_{\mathrm{L}} - D\kappa\right) \mathbf{n}_{\mathrm{F}} \cdot \nabla G = 0, \tag{2.3}$$

$$\rho \frac{\partial c}{\partial t} + \rho \mathbf{u} \cdot \nabla c - \nabla \cdot (\rho D \nabla c) = \dot{\omega}_c, \tag{2.4}$$

where ρ denotes the density, $\mathbf{u}$ the velocity, p_{hyd} the hydrodynamic pressure, μ the viscosity, $\mathbf{I}$ the identity tensor, $\mathbf{g}$ the gravity-force vector, G the level-set function, s_{L} the laminar burning velocity, D the (kinematic) diffusivity, $\kappa = \nabla \cdot \mathbf{n}_{\mathrm{F}}$ the curvature, $\mathbf{n}_{\mathrm{F}} = -\nabla G / |\nabla G|$ the normal to the flame front, c the progress variable, and $\dot{\omega}_c$ the reaction-rate term. The notation $\varepsilon' (\mathbf{u}) = \varepsilon (\mathbf{u}) - (1/3) (\nabla \cdot \mathbf{u}) \mathbf{I}$ including the rate-of-deformation tensor $\varepsilon (\mathbf{u}) = \frac{1}{2} \left(\nabla \mathbf{u} + \left(\nabla \mathbf{u}^{\mathrm{T}}\right)\right)$ is used. The subscript "u" denotes values in the unburned phase, whereas subscript "b" denotes values in the burned phase. Appropriate initial and boundary conditions need to be defined for the system of equations above; however, they will be omitted in the following for the sake of brevity.

2.1.1. *Alternative forms of mass-conservation equation and density evaluation*

The mass-conservation equation may be rewritten either as

$$\nabla \cdot \mathbf{u} = \frac{\rho_{\mathrm{u}} - \rho_{\mathrm{b}}}{\rho} \left(\frac{\partial c}{\partial t} + \mathbf{u} \cdot \nabla c\right), \tag{2.5}$$

when the validity of the Bray-Moss-Libby (BML) hypothesis (see, e.g., Bray & Moss (1977)) is assumed, with the implication that

$$\rho = \rho_{\mathrm{u}} + c \left(\rho_{\mathrm{b}} - \rho_{\mathrm{u}}\right). \tag{2.6}$$

Alternatively, it may be rewritten as

$$\nabla \cdot \mathbf{u} = \frac{\left(\rho_{\mathrm{u}} - \rho_{\mathrm{b}}\right) \rho}{\rho_{\mathrm{u}} \rho_{\mathrm{b}}} \left(\frac{\partial c}{\partial t} + \mathbf{u} \cdot \nabla c\right), \tag{2.7}$$

if density evaluated via the equation of state for an ideal gas, $\rho = p_{\mathrm{the}} / (RT)$, with thermodynamic pressure p_{the} (assumed constant here), gas constant R and temperature T, which is equivalent to

$$\rho = \frac{\rho_{\mathrm{u}} \rho_{\mathrm{b}}}{\rho_{\mathrm{b}} + c \left(\rho_{\mathrm{u}} - \rho_{\mathrm{b}}\right)}. \tag{2.8}$$

In the following, the validity of the BML hypothesis is assumed; it is straightforward to obtain the alternative version by using the respective equation of state.

2.1.2. *Interface conditions for G-equation*

Jump conditions at the flame front Γ_{int}, which represents the interface between burned and unburned phases, may be derived from mass and momentum conservation across the

interface, as originally done in the context of hydrodynamic theory, e.g., in Matalon & Matkowsky (1982):

$$[\mathbf{u}\cdot\mathbf{n}] = -M[\rho^{-1}] \qquad \text{on } \Gamma_{\text{int}}, \tag{2.9}$$

$$[\mathbf{u}\cdot\mathbf{t}_1] = 0 \qquad \text{on } \Gamma_{\text{int}}, \tag{2.10}$$

$$[\mathbf{u}\cdot\mathbf{t}_2] = 0 \qquad \text{on } \Gamma_{\text{int}}, \tag{2.11}$$

$$[p] = M^2[\rho^{-1}] \qquad \text{on } \Gamma_{\text{int}}, \tag{2.12}$$

where the operator $[x] = x_{\text{b}} - x_{\text{u}}$ defines the jump in a quantity across the interface, $\mathbf{t}_1$ and $\mathbf{t}_2$ represent the tangential vectors at the interface and M denotes the mass flux across the flame front:

$$M = \rho_{\text{b}}\left(\mathbf{u}_{\text{f}}\cdot\mathbf{n} - \mathbf{u}_{\text{b}}\cdot\mathbf{n}\right) = \rho_{\text{u}}\left(\mathbf{u}_{\text{f}}\cdot\mathbf{n} - \mathbf{u}_{\text{u}}\cdot\mathbf{n}\right) = \rho_{\text{u}} s_{\text{L}}. \tag{2.13}$$

Here, the absolute flame speed (in a fixed reference frame) is given by $\mathbf{u}_{\text{f}}\cdot\mathbf{n}$. In hydrodynamic theory, the effect of viscosity at the flame front is not taken into account. Including viscosity, the fourth interface condition changes towards

$$[\sigma\cdot\mathbf{n}] = M[\mathbf{u}] \qquad \text{on } \Gamma_{\text{int}}, \tag{2.14}$$

with the stress tensor denoted by σ.

2.1.3. *Chemical kinetics*

As in Gravemeier & Wall (2010*b*), three alternative formulations for the reactive right-hand-side term of Eq. (2.4) may be considered: Arrhenius chemical kinetics, a simplified chemical-kinetics formulation proposed in Ferziger & Echekki (1993), and a slightly modified version of the latter as proposed in Poinsot & Veynante (2005). Defining a reaction coefficient σ, the progress-variable equation may be reformulated in a schematic form for a transient convection-diffusion-reaction equation with non-zero right-hand side as follows:

$$\rho\frac{\partial c}{\partial t} + \rho\mathbf{u}\cdot\nabla c - \nabla\cdot(\rho D\nabla c) + \rho\sigma c = \rho\sigma. \tag{2.15}$$

This form of the progress-variable equation will be used below.

2.2. *Extended algebraic variational multiscale-multigrid method*

The algebraic variational multiscale-multigrid method (AVM^3) was originally proposed for large-eddy simulation of turbulent incompressible flow in Gravemeier *et al.* (2010) and extended towards turbulent variable-density flow at low Mach number in Gravemeier & Wall (2010*a*). In this section, starting from a variational formulation of the system of equations and an appropriate scale decomposition, the final formulation of the AVM^3 will be presented as a result of two modeling steps. At the end of the section, an appropriate definition of the compatibility condition and the characteristic flame thickness will be addressed, respectively.

2.2.1. *Variational formulation and scale decomposition*

As the first step, to obtain a variational formulation of the system of equations, appropriate solution function spaces $\mathcal{S}_{\{p,\mathbf{u},G,c\}}$ for p_{hyd}, $\mathbf{u}$, G and c as well as weighting function spaces $\mathcal{V}_{\{p,\mathbf{u},G,c\}}$ for the respective weighting functions q, $\mathbf{v}$, r and w are assumed. The variational formulation is given as follows: find $p_{\text{hyd}} \in \mathcal{S}_p$, $\mathbf{u} \in \mathcal{S}_{\mathbf{u}}$, $G \in \mathcal{S}_G$ and $c \in \mathcal{S}_c$

such that

$$(q, \nabla \cdot \mathbf{u}) = \left(q, \frac{\rho_\mathrm{u} - \rho_\mathrm{b}}{\rho} \left(\frac{\partial c}{\partial t} + \mathbf{u} \cdot \nabla c \right) \right) \ \forall\, q \in \mathcal{V}_p, \tag{2.16}$$

$$\left(\mathbf{v}, \rho \frac{\partial \mathbf{u}}{\partial t} \right) + (\mathbf{v}, \rho \mathbf{u} \cdot \nabla \mathbf{u}) - (\nabla \cdot \mathbf{v}, p_\mathrm{hyd}) + (\varepsilon(\mathbf{v}), 2\mu\varepsilon'(\mathbf{u})) = (\mathbf{v}, \rho \mathbf{g}) \ \forall\, \mathbf{v} \in \mathcal{V}_\mathbf{u}, \tag{2.17}$$

$$\left(r, \rho \frac{\partial G}{\partial t} \right) + (r, \rho \mathbf{u} \cdot \nabla G) + (r, \rho_\mathrm{u} s_\mathrm{L} \mathbf{n}_\mathrm{F} \cdot \nabla G) + (\nabla r, \rho_\mathrm{u} D \nabla G) = 0 \quad \forall\, r \in \mathcal{V}_G, \tag{2.18}$$

$$\left(w, \rho \frac{\partial c}{\partial t} \right) + (w, \rho \mathbf{u} \cdot \nabla c) + (\nabla w, \rho D \nabla c) + (w, \rho \sigma c) = (w, \rho \sigma) \ \forall\, w \in \mathcal{V}_c, \tag{2.19}$$

where $(\cdot, \cdot) = (\cdot, \cdot)_\Omega$ denotes the L_2-inner product on Ω. Note that the last term on the left-hand side in Eq. (2.18) is integrated by parts, exploiting that $\mathbf{n}_\mathrm{F} = -\nabla G / |\nabla G|$ and $\kappa = \nabla \cdot \mathbf{n}_\mathrm{F}$.

A variational projection for separating resolved and unresolved scales, as described, e.g., in Gravemeier & Wall (2010*a*,*b*), is assumed here. Hence, hydrodynamic pressure, velocity, G- and progress-variable fields are first decomposed via variational projection into two scale ranges, resolved and unresolved (or subgrid) scales, as

$$p_\mathrm{hyd} = p^h_\mathrm{hyd} + \hat{p}_\mathrm{hyd}, \ \mathbf{u} = \mathbf{u}^h + \hat{\mathbf{u}}, \ G = G^h + \hat{G}, \ c = c^h + \hat{c}, \tag{2.20}$$

where h indicates the characteristic element length of the discretization. The resolved scales are the scales which are resolvable by this characteristic length of the discretization; consequently, all smaller scales are considered unresolved scales. A three-scale decomposition of the velocity further separating the resolved-scale part into a large resolved and a small resolved is required for the small-scale subgrid-viscosity term to be added below:

$$\mathbf{u} = \underbrace{\mathbf{u}^{3h} + \delta\mathbf{u}^h}_{\mathbf{u}^h} + \hat{\mathbf{u}}. \tag{2.21}$$

2.2.2. *Modeling step 1: residual-based subgrid-scale modeling*

The subgrid-scale parts of hydrodynamic pressure, velocity, G- and progress-variable field are approximated in an elementwise manner based on the resolved-scale parts. Hence, in each element, the subgrid-scale parts are given as

$$\hat{p}_\mathrm{hyd} = -\tau_\mathrm{C} \mathcal{R}^h_\mathrm{C}, \quad \hat{\mathbf{u}} = -\tau_\mathrm{M} \mathcal{R}^h_\mathrm{M}, \quad \hat{G} = -\tau_\mathrm{G} \mathcal{R}^h_\mathrm{G}, \quad \hat{c} = -\tau_\mathrm{P} \mathcal{R}^h_\mathrm{P}. \tag{2.22}$$

The discrete residuals of continuity, momentum G- and progress-variable equation read

$$\mathcal{R}^h_\mathrm{C} = \nabla \cdot \mathbf{u}^h - \frac{\rho_\mathrm{u} - \rho_\mathrm{b}}{\rho^h} \left(\frac{\partial c^h}{\partial t} + \mathbf{u}^h \cdot \nabla c^h \right), \tag{2.23}$$

$$\mathcal{R}^h_\mathrm{M} = \rho^h \frac{\partial \mathbf{u}^h}{\partial t} + \rho^h \mathbf{u}^h \cdot \nabla \mathbf{u}^h + \nabla p^h_\mathrm{hyd} - \nabla \cdot \left(2\mu^h \varepsilon'\left(\mathbf{u}^h\right) \right) - \rho^h \mathbf{g}, \tag{2.24}$$

$$\mathcal{R}^h_\mathrm{G} = \rho^h \frac{\partial G^h}{\partial t} + \rho^h \mathbf{u}^h \cdot \nabla G^h + \rho_\mathrm{u} \left(s_\mathrm{L} - D\kappa^h \right) \mathbf{n}^h_\mathrm{F} \cdot \nabla G^h, \tag{2.25}$$

$$\mathcal{R}^h_\mathrm{P} = \rho^h \frac{\partial c^h}{\partial t} + \rho^h \mathbf{u}^h \cdot \nabla c^h - \nabla \cdot \left(\rho D \nabla c^h \right) + \rho^h \sigma^h \left(c^h - 1 \right). \tag{2.26}$$

The algebraic parameters for the respective conservation equations are defined as follows:

$$\tau_{\mathrm{C}} = \frac{1}{\tau_{\mathrm{M}} \operatorname{tr}(\mathbf{G})}, \tag{2.27}$$

$$\tau_{\mathrm{M}} = \frac{1}{\sqrt{\left(\frac{2\rho^h}{\Delta t}\right)^2 + (\rho^h \mathbf{u}^h) \cdot \mathbf{G} (\rho^h \mathbf{u}^h) + C_{\mathrm{I}} \mu^2 \mathbf{G} : \mathbf{G}}}, \tag{2.28}$$

$$\tau_{\mathrm{G}} = \frac{1}{\sqrt{\left(\frac{2\rho^h}{\Delta t}\right)^2 + (\rho^h \mathbf{u}^h) \cdot \mathbf{G} (\rho^h \mathbf{u}^h) + \left(\rho_{\mathrm{u}} s_{\mathrm{L}} \mathbf{n}_{\mathrm{F}}^h\right) \cdot \mathbf{G} \left(\rho_{\mathrm{u}} s_{\mathrm{L}} \mathbf{n}_{\mathrm{F}}^h\right) + C_{\mathrm{I}} \left(\rho_{\mathrm{u}} D\right)^2 \mathbf{G} : \mathbf{G}}}, \tag{2.29}$$

$$\tau_{\mathrm{P}} = \frac{1}{\sqrt{\left(\rho^h \left(\frac{2}{\Delta t} + \sigma^h\right)\right)^2 + (\rho^h \mathbf{u}^h) \cdot \mathbf{G} (\rho^h \mathbf{u}^h) + C_{\mathrm{I}} \left(\rho^h D\right)^2 \mathbf{G} : \mathbf{G}}}, \tag{2.30}$$

where

$$G_{ij} = \sum_{k=1}^{3} \frac{\partial \xi_k}{\partial x_i} \frac{\partial \xi_k}{\partial x_j}, \tag{2.31}$$

utilizing the coordinate system ξ of the element parent domain. The time-step size of the temporal discretization of the problem formulation is denoted by Δt, and C_{I} is a positive constant independent of the characteristic element length h. Parameter definition Eq. (2.28) represents a formulation for variable-density flow problems as already used in Gravemeier & Wall (2010*a*), which is based on the parameter definition for incompressible flow proposed in Bazilevs *et al.* (2007). Parameter definition Eq. (2.27) was recently proposed in Bazilevs & Akkerman (2010) as a slight modification to that in Bazilevs *et al.* (2007).

2.2.3. *Modeling step 2: small-scale subgrid-viscosity term*

The key ingredient of the AVM^3 is a small-scale subgrid-viscosity term, which is based on the physical reasoning that energy transport in turbulent flow occurs mainly between scales of similar size. The present model should account in particular for the effect of unresolved scales on the small resolved scales. The subgrid viscosity $\mu_{\mathrm{T}}^{\delta h}$ is assumed to depend only on the small resolved scales. It is defined by a modified (constant-coefficient) Smagorinsky model as

$$\mu_{\mathrm{T}}^{\delta h} = \rho^h \left(C_{\mathrm{S}} h\right)^2 \left|\varepsilon(\delta \mathbf{u}^h)\right|, \tag{2.32}$$

with C_{S} denoting the Smagorinsky constant and $\left|\varepsilon(\delta \mathbf{u}^h)\right| = \sqrt{2\varepsilon(\delta \mathbf{u}^h) : \varepsilon(\delta \mathbf{u}^h)}$ the norm of the rate-of-deformation tensor based on the small-scale velocity. The Smagorinsky constant C_{S} is chosen to be 0.1 in various preceding studies (e.g., Gravemeier *et al.* (2010); Gravemeier & Wall (2010*a*)); the application of a constant-coefficient Smagorinsky model based on the small resolved scales and with this particular choice for the parameter yielded very good results for various test cases in those studies. Usually, no parameter tuning is performed to keep the modeling as simple as possible.

Plain aggregation algebraic multigrid (PA-AMG) is used for generating prolongation and restriction (i.e., level-transfer) operator matrices based on algebraic principles. According to this, a prolongation operator matrix $\mathbf{P}_{3h}^h$ is generated. The restriction operator matrix $\mathbf{R}_h^{3h}$ is chosen to be the transpose of the prolongation operator matrix. A scale-separating operator matrix is defined as $\mathbf{S}_h^{3h} = \mathbf{P}_{3h}^h \mathbf{R}_h^{3h}$ and then used to ensure that the

subgrid-viscosity term is directly acting only on the smaller of the resolved scales. The reader is referred to Gravemeier *et al.* (2010); Gravemeier & Wall (2010*a*) for elaboration and to Gravemeier (2006) for a similar approach in the context of a finite volume method using geometric instead of algebraic multigrid.

2.2.4. *Extended finite element approach*

As a methodical framework for taking into account interfaces within a finite element method on fixed meshes, the eXtended Finite Element Method (XFEM) was developed, at first for problems of crack growth in solid mechanics; see, e.g., Belytschko & Black (1999). Later on, XFEMs were developed for and applied to other problem configurations featuring interfaces. To the best of the author's knowledge, the first and so far only development and application of an XFEM to premixed combustion was recently reported in van der Bos & Gravemeier (2009).

In order to correctly reproduce discontinuous solution fields as required by the G-equation concept, the standard finite element method is extended by enriching the function spaces with appropriate discontinuous functions. In the case of the problem under consideration, a (symmetric) Heaviside function is used to represent jumps across the interface, that is, the flame front:

$$H(\mathbf{x},t) = \begin{cases} -1 & \text{if } G(\mathbf{x},t) \leq 0 \\ 1 & \text{if } G(\mathbf{x},t) > 0. \end{cases} \tag{2.33}$$

The function space is only locally enriched (i.e., in the vicinity of the flame front). Furthermore, the partition-of-unity concept is retained. If an element is intersected by the interface (i.e., $G(\mathbf{x}) = 0$ within the element), all nodes belonging to this element are enriched by additional degrees of freedom. For example, an enriched velocity solution is given as

$$\mathbf{u}^h(\mathbf{x},t) = \sum_{A\in\eta} N_A(\mathbf{x})\,\mathbf{u}_A(t) + \sum_{\tilde{A}\in\eta_{\text{enr}}} N_{\tilde{A}}(\mathbf{x})\,\psi_{\tilde{A}}(\mathbf{x},t)\,\tilde{\mathbf{u}}_{\tilde{A}}(t)\,, \tag{2.34}$$

where N_A, $\mathbf{u}_A$ and $\tilde{\mathbf{u}}_A$ denote the finite element shape function, standard velocity degrees of freedom and enriched velocity degrees of freedom at node A, respectively. The set of all nodes of the discretization is indicated by η, and the particular set of nodes with enriched degrees of freedom, which is generally a subset of η, by η_{enr}. Hence, the resulting solution $\mathbf{u}^h(\mathbf{x})$ may be interpreted as a superposition of standard and enriched degrees of freedom. In the present case, the enrichment function is given as

$$\psi_{\tilde{A}}(\mathbf{x},t) = H\left(G(\mathbf{x},t)\right) - H\left(G(\mathbf{x}_{\tilde{A}},t)\right). \tag{2.35}$$

Another type of enrichment functions in the form of a "kink" enrichment is used, for instance, for two-phase flow problems as considered in Rasthofer *et al.* (2010).

Integration over intersected elements and along the flame front is performed by means of integration cells. A sub-tetrahedralization procedure results in cells that lie on one side of the interface and together add up to the element volume. In doing so, the discontinuous flow field can be integrated correctly.

2.2.5. *Final formulation*

The AVM^3 is finally given as follows: find $p^h_{\text{hyd}} \in \mathcal{S}^h_p$, $\mathbf{u}^h \in \mathcal{S}^h_{\mathbf{u}}$, $G^h \in \mathcal{S}^h_G$ and $c^h \in \mathcal{S}^h_c$ such that

$$\left(q^h, \nabla\cdot\mathbf{u}^h\right) + \sum_{e=1}^{n_{\text{el}}} \left(\nabla q^h, \tau_{\text{M}}\mathcal{R}^h_{\text{M}}\right)_{\Omega^e}$$

$$= \left(q^h, \tfrac{\rho_\mathrm{u}-\rho_\mathrm{b}}{\rho^h}\left(\tfrac{\partial c^h}{\partial t} + \mathbf{u}^h \cdot \nabla c^h\right)\right) \quad \forall\, q^h \in \mathcal{V}_p^h, \tag{2.36}$$

$$\begin{aligned}
&\left(\mathbf{v}^h, \rho^h \tfrac{\partial \mathbf{u}^h}{\partial t}\right) + \left(\mathbf{v}^h, \rho^h \mathbf{u}^h \cdot \nabla \mathbf{u}^h\right) - \left(\nabla \cdot \mathbf{v}^h, p^h_\mathrm{hyd}\right) + \left(\varepsilon\left(\mathbf{v}^h\right), 2\mu\varepsilon'\left(\mathbf{u}^h\right)\right) \\
&+ \left(\varepsilon\left(\delta\mathbf{v}^h\right), 2\mu_\mathrm{T}^{\delta h}\varepsilon'\left(\delta\mathbf{u}^h\right)\right) + \sum_{e=1}^{n_\mathrm{el}} \left(\nabla \cdot \mathbf{v}^h, \tau_\mathrm{C}\mathcal{R}^h_\mathrm{C}\right)_{\Omega^e} + \sum_{e=1}^{n_\mathrm{el}} \left(\rho^h \mathbf{u}^h \cdot \nabla \mathbf{v}^h, \tau_\mathrm{M}\mathcal{R}^h_\mathrm{M}\right)_{\Omega^e} \\
&= \left(\mathbf{v}^h, \rho^h \mathbf{g}\right) \quad \forall\, \mathbf{v}^h \in \mathcal{V}^h_\mathbf{u},
\end{aligned} \tag{2.37}$$

$$\begin{aligned}
&\left(w^h, \rho \tfrac{\partial G^h}{\partial t}\right) + \left(w^h, \rho^h \mathbf{u}^h \cdot \nabla G^h\right) + \left(w^h, \rho_\mathrm{u} s_\mathrm{L} \mathbf{n}^h_\mathrm{F} \cdot \nabla G^h\right) + \left(\nabla w^h, \rho_\mathrm{u} D \nabla G^h\right) \\
&+ \sum_{e=1}^{n_\mathrm{el}} \left(\rho^h \mathbf{u}^h \cdot \nabla w^h, \tau_\mathrm{G}\mathcal{R}^h_\mathrm{G}\right)_{\Omega^e} + \sum_{e=1}^{n_\mathrm{el}} \left(\rho_\mathrm{u} s_\mathrm{L} \mathbf{n}^h_\mathrm{F} \cdot \nabla w^h, \tau_\mathrm{G}\mathcal{R}^h_\mathrm{G}\right)_{\Omega^e} \\
&= 0 \quad \forall\, w^h \in \mathcal{V}^h_G,
\end{aligned} \tag{2.38}$$

$$\begin{aligned}
&\left(w^h, \rho^h \tfrac{\partial c^h}{\partial t}\right) + \left(w^h, \rho^h \mathbf{u}^h \cdot \nabla c^h\right) + \left(\nabla w^h, \rho D \nabla c^h\right) + \left(w^h, \rho^h \sigma^h c^h\right) \\
&+ \sum_{e=1}^{n_\mathrm{el}} \left(\rho^h \mathbf{u}^h \cdot \nabla w^h, \tau_\mathrm{P}\mathcal{R}^h_\mathrm{P}\right)_{\Omega^e} - \sum_{e=1}^{n_\mathrm{el}} \left(\rho^h \sigma^h w^h, \tau_\mathrm{P}\mathcal{R}^h_\mathrm{P}\right)_{\Omega^e} \\
&= \left(w^h, \rho^h \sigma^h\right) \quad \forall\, w^h \in \mathcal{V}^h_c.
\end{aligned} \tag{2.39}$$

The following modeling terms appear in this formulation, which are all defined as sums over all element domains Ω^e, where n_el denotes the number of elements of the discretization, except for the small-scale subgrid-viscosity term:

- a Pressure-Stabilizing Petrov-Galerkin (PSPG) term (last term on the left-hand side of Eq. (2.36),
- a small-scale subgrid-viscosity term (fifth term on the left-hand side of Eq. (2.37)),
- a grad-div term (sixth term on the left-hand side of Eq. (2.37)),
- Streamline Upwind Petrov-Galerkin (SUPG) terms (last term on the left-hand side of Eq. (2.37), fifth and sixth term on the left-hand side of Eq. (2.38), fifth term on the left-hand side of Eq. (2.39)),
- a reactive subgrid-scale term (last term on the left-hand side of Eq. (2.39)).

The negative sign in front of the reactive subgrid-scale term is due to the negative adjoint differential operator as arising from a variational multiscale formulation; see, e.g., Hughes *et al.* (1998).

The present formulation turned out to be the most robust version of the AVM^3 as a result of various test examples in Gravemeier *et al.* (2010); Gravemeier & Wall (2010*a*), among others. Alternative formulations including other terms and/or excluding some of the present terms are easily achievable within the methodical framework.

2.2.6. *Compatibility condition and characteristic flame thickness*

In Moureau *et al.* (2009), the following general form of a compatibility condition was proposed:

$$\int_{-\infty}^{+\infty} \overline{\dot{\omega}}_c \, \mathrm{d}x_n = \rho_\mathrm{u} s_\Delta, \tag{2.40}$$

where $\overline{\dot{\omega}}_c$ denotes the filtered form of the reaction-rate term, x_n the coordinate in the direction normal to the flame front, Δ the characteristic filter size and s_Δ an (effec-

tive) burning velocity, which depends on this filter size. From this general condition, a particular formulation for $\overline{\dot{\omega}}_c$ ensuring a realizable closure of the filtered form of the progress-variable equation was developed and used in Moureau *et al.* (2009).

The present numerical approach is based on variational projection in lieu of filtering; see, e.g., Gravemeier & Wall (2010*b*) for some brief remarks on the differences in the present context. As a result, instead of the filter-based burning velocity s_Δ, a burning velocity based on the characteristic element length of the discretization s^h is defined in analogy as follows:

$$s^h = s_\mathrm{L} + s_\mathrm{T} - D\kappa^h - D_{\mathrm{T},G}\kappa^h, \tag{2.41}$$

where s_T denotes the turbulent burning velocity and $D_{\mathrm{T},G}$ the turbulent diffusivity applied to the G-equation. For computing the turbulent burning velocity, definitions such as the ones provided in Peters (1999) or later in Pitsch (2005) may be used.

Another important value is the characteristic flame thickness, which may be defined for the present case in analogy with the definition in Moureau *et al.* (2009) as

$$l_\mathrm{f}^h = \frac{D_{\mathrm{T},c}}{s^h}, \tag{2.42}$$

where $D_{\mathrm{T},c}$ represents the turbulent diffusivity applied to the progress-variable equation. This length scale will be used in the computations for evaluating the ratio of the characteristic flame thickness on the one hand, and the characteristic element length of the discretization on the other hand. If

$$l_\mathrm{f}^h < kh, \tag{2.43}$$

with k denoting a constant which needs to be defined *a priori*, the characteristic flame thickness is smaller than the characteristic length scale of the discretization, and the flame cannot be resolved on the present discretization; thus, an additional solution of the progress-variable is not required, and the modeling may be restricted to a "pure" application of the G-equation concept. Otherwise, the complete combined modeling procedure will be applied.

3. Future Plans

The method presented in Section 2.2 will be implemented and tested for problems of turbulent premixed combustion. However, two goals particularly related to the XFEM/G-equation approach must first be satisfied:

- the development of an adequate time-integration scheme for the XFEM and
- the development of an efficient approach to enforcing the interface conditions for XFEM applications to three-dimensional problem configurations.

These two issues are the subjects of ongoing research efforts within the author's Emmy Noether research group as well as by a variety of researchers worldwide working on XFEMs, since they are both not restricted to premixed combustion problems. In the following, both issues will be briefly addressed.

Time dependencies of XFEM-based functions such as Eq. (2.34) and functions in a standard FEM are different. When employing a semi-discrete time-discretization procedure in a standard FEM, the shape functions N_A are generally constant in time, and only the nodal values (e.g., $\mathbf{u}_i$) are time-dependent, as indicated in Eq. (2.34). In contrast, additional time dependencies have to be taken into account in the XFEM when moving interfaces are considered. While the standard shape functions are still constant

in time, the enriched shape functions are time-dependent, since they result from products of standard shape functions and enrichment functions $\psi(\mathbf{x}, t)$, with the latter being time-dependent. Moreover, as only intersected elements are enriched, there are generally nodes which were enriched at the last time step but not at the current one, and vice versa. That is, a consecutive process of adding and removing enriched degrees of freedom takes place during a simulation. This process has to be adequately accounted for in the time-integration scheme used in an XFEM. A convincing time-integration for XFEMs based on semi-discretization has not yet appeared in the literature, to the best of the author's knowledge. In the author's own preceding work, together with various co-workers, quasi-static enrichments were developed and used in Rasthofer *et al.* (2010), and simplified time-integration schemes were used in van der Bos & Gravemeier (2009). The development of a more universally valid XFEM-based time-integration scheme is currently under way.

The challenge of taking into account embedded interfaces within the XFEM has been addressed by several authors, proposing different procedures. It has to be emphasized that the moving interface usually intersects the finite elements such that the application of interface conditions merely at element nodes is not possible. Formulations employing Lagrange multipliers were developed for two-dimensional problems, e.g., in van der Bos & Gravemeier (2009). Finding appropriate Lagrange multipliers for two-dimensional problems is rather challenging. For three-dimensional problems, the challenge is considerably enhanced, if it is indeed possible to find such multipliers. Alternative methods were proposed where Lagrange multipliers are not required on an interface mesh but are embedded into the intersected elements of the basic discretizations. Recently, promising new approaches based on Nitsche's method and a mixed-hybrid formulation were proposed in Dolbow & Harari (2009) and Gerstenberger & Wall (2010), respectively, intended to circumvent drawbacks of the aforementioned Lagrange-multiplier-based approaches. These methods, which are not restricted to particular problems but rather are considered suitable for a wide range of problems in computational mechanics, are currently being investigated for their suitability for the present problem of premixed combustion.

Acknowledgments

The support of the author's research stay at the Center for Turbulence Research by the Alexander von Humboldt-Foundation via a Feodor Lynen Alumni Fellowship is gratefully acknowledged.

REFERENCES

Bazilevs, Y. & Akkerman, I. 2010 Large eddy simulation of turbulent taylorcouette flow using isogeometric analysis and the residual-based variational multiscale method. *J. Comput. Phys.* **229**, 3402–3414.

Bazilevs, Y., Calo, V. M., Cottrell, J. A., Hughes, T. J. R., Reali, A. & Scovazzi, G. 2007 Variational multiscale residual-based turbulence modeling for large eddy simulation of incompressible flows. *Comput. Methods Appl. Mech. Engrg.* **197**, 173–201.

Belytschko, T. & Black, T. 1999 Elastic crack growth in finite elements with minimal remeshing. *Int. J. Numer. Meth. Engng.* **45**, 601–620.

Bilger, R. W., Pope, S. B., Bray, K. N. C. & Driscoll, J. F. 2005 Paradigms in turbulent combustion research. *Proc. Combust. Inst.* **30**, 21–42.

Boger, M., Veynante, D., Boughanem, H. & Trouvé, A. 1998 Direct numerical simulation analysis of flame surface density concept for large eddy simulation of turbulent premixed combustion. *Proc. Combust. Inst.* **27**, 917–925.

van der Bos, F. & Gravemeier, V. 2009 Numerical simulation of premixed combustion using an enriched finite element method. *J. Comput. Phys.* **228**, 3605–3624.

Bray, K. N. C. & Moss, J. B. 1977 A unified statistical model of the premixed turbulent flame. *Acta Astronaut.* **4**, 291–319.

Dolbow, J. & Harari, I. 2009 An efficient finite element method for embedded interface problems. *Int. J. Numer. Meth. Engng.* **78**, 229–252.

Ferziger, J. H. & Echekki, T. 1993 A simplified reaction rate model and its application to the analysis of premixed flames. *Combust. Sci. Technol.* **89**, 293–315.

Gerstenberger, A. & Wall, W. A. 2010 An embedded dirichlet formulation for 3d continua. *Int. J. Numer. Meth. Engng.* **82**, 537–563.

Gravemeier, V. 2006 Scale-separating operators for variational multiscale large eddy simulation of turbulent flows. *J. Comput. Phys.* **212**, 400–435.

Gravemeier, V., Gee, M. W., Kronbichler, M. & Wall, W. A. 2010 An algebraic variational multiscale-multigrid method for large eddy simulation of turbulent flow. *Comput. Methods Appl. Mech. Engrg.* **199**, 853–864.

Gravemeier, V. & Wall, W. A. 2010*a* An algebraic variational multiscale-multigrid method for large-eddy simulation of turbulent variable-density flow at low mach number. *J. Comput. Phys.* **229**, 6047–6070.

Gravemeier, V. & Wall, W. A. 2010*b* Variational multiscale methods for premixed combustion based on a progress-variable approach. Combust. Flame, in press.

Hartmann, D., Meinke, M. & Schröder, W. 2010 An adaptive dual-mesh method for premixed combustion using the level-set approach. *AIAA Paper* **2010-1068**.

Hawkes, E. R. & Cant, R. S. 2000 A flame surface density approach to large-eddy simulation of premixed turbulent combustion. *Proc. Combust. Inst.* **28**, 51–58.

Hughes, T. J. R., Feijoo, G., Mazzei, L. & Quincy, J.-B. 1998 The variational multiscale method–a paradigm for computational mechanics. *Comput. Methods Appl. Mech. Engrg.* **166**, 3–24.

Janicka, J. & Sadiki, A. 2005 Large eddy simulation of turbulent combustion systems. *Proc. Combust. Inst.* **30**, 537–547.

Matalon, M. & Matkowsky, B. J. 1982 Flames as gasdynamic discontinuities. *J. Fluid Mech.* **124**, 239–259.

Moureau, V., Fiorina, B. & Pitsch, H. 2009 A level set formulation for premixed combustion les considering the turbulent flame structure. *Combust. Flame* **156**, 801–812.

Osher, S. & Fedkiw, R. 2003 *Level set methods and dynamic implicit surfaces*. Springer-Verlag.

Peters, N. 1999 The turbulent burning velocity for large-scale and small-scale turbulence. *J. Fluid Mech.* **384**, 107–132.

Peters, N. 2000 *Turbulent combustion*. Cambridge University Press.

Pitsch, H. 2005 A consistent level set formulation for large-eddy simulation of premixed turbulent combustion. *Combust. Flame* **143**, 587–598.

Pitsch, H. 2006 Large-eddy simulation of turbulent combustion. *Ann. Rev. Fluid Mech.* **38**, 453–482.

Poinsot, T. & Veynante, D. 2005 *Theoretical and numerical combustion*. R. T. Edwards.

Rasthofer, U., Henke, F., Wall, W. A. & Gravemeier, V. 2010 An extended variational multiscale method for two-phase flow. Preprint, submitted for publication in Comput. Methods Appl. Mech. Engrg.

Williams, F. A. 1985 Turbulent combustion. In *The Mathematics of Combustion* (ed. J. Buckmaster), pp. 97–131. SIAM.